STEM CELLS AND DEVELOPMENT
Volume 22, Number 12, 2013

DOI: 10.1089/scd.2012.0688

Functional Tooth Restoration by Allogeneic Mesenchymal Stem Cell-Based Bio-Root Regeneration in Swine

Fulan Wei,[1] Tieli Song,[1] Gang Ding,[1] Junji Xu,[1] Yi Liu,[1] Dayong Liu,[1] Zhipeng Fan,[1] Chunmei Zhang,[1] Songtao Shi,[2] and Songlin Wang[1,3]

Our previous proof-of-concept study showed the feasibility of regenerating the dental stem cell-based bioengineered tooth root (bio-root) structure in a large animal model. Here, we used allogeneic dental mesenchymal stem cells to regenerate bio-root, and then installed a crown on the bio-root to restore tooth function. A root shape hydroxyapatite tricalcium phosphate scaffold containing dental pulp stem cells was covered by a Vc-induced periodontal ligament stem cell sheet and implanted into a newly generated jaw bone implant socket. Six months after implantation, a prefabricated porcelain crown was cemented to the implant and subjected to tooth function. Clinical, radiological, histological, ultrastructural, systemic immunological evaluations and mechanical properties were analyzed for dynamic changes in the bio-root structure. The regenerated bio-root exhibited characteristics of a normal tooth after 6 months of use, including dentinal tubule-like and functional periodontal ligament-like structures. No immunological response to the bio-roots was observed. We developed a standard stem cell procedure for bio-root regeneration to restore adult tooth function. This study is the first to successfully regenerate a functional bio-root structure for artificial crown restoration by using allogeneic dental stem cells and Vc-induced cell sheet, and assess the recipient immune response in a preclinical model.

Introduction

Tooth loss due to periodontal disease, dental caries, trauma, or a variety of genetic disorders continues to adversely affect most adults in their lives. Regenerative medicine and tissue engineering technologies offer promising therapies for medicine and dentistry [1,2]. Recent advances in dental stem cell biotechnology and cell-based murine tooth regeneration have encouraged researchers to explore the potential for regenerating living functional teeth [3]. However, owing to the complexity of human tooth growth and development, much more researches were needed to regenerate a whole tooth structure, including enamel, dentin/pulp complex, and periodontal tissues as a functional entity. A tooth root that can support a natural or artificial crown is the most important part of the tooth in maintaining tooth functions [4]. Previously, we showed the potential that autologous dental stem cells may be able to form a bioengineered tooth root (bio-root) for temporally supporting artificial crowns in a miniature pig (minipig) as proof of concept preliminary data [5,6]. However, most patients are aged, and sources of autologous dental stem cells are limited. Due to the low immunogenicity and immunomodulation function, allogeneic mesenchymal stem cells (MSCs) could treat systemic lupus erythematosus mice/human [7], Sjögren's syndrome [8], and periodontitis-induced bone defects [9], suggesting that allogeneic MSCs have the potential for dental tissue regeneration. In the present study, we regenerated a functional bio-root using allogeneic dental MSCs and Vc-induced cell sheet, developed a standard stem cell procedure for bio-root regeneration and function tooth restoration in a swine model.

Design and Methods

Animals

This study was reviewed and approved by the Animal Care and Use Committees of the Capital Medical University. Eighteen inbred miniature pigs (minipigs) aged 18 months and weighing 50–60 kg were obtained from the Institute of Animal Science at the Chinese Agriculture University. Animals were housed under conventional conditions with free access to water and food. These animals were randomly divided into three groups: (1) the hydroxyapatite tricalcium

[1]Molecular Laboratory for Gene Therapy and Tooth Regeneration, Beijing Key Laboratory of Tooth Regeneration and Function Reconstruction, Capital Medical University School of Stomatology, Beijing, People's Republic of China.
[2]The Center for Craniofacial Molecular Biology, Herman Ostrow School of Dentistry, University of Southern California Los Angeles, Los Angeles, California.
[3]Department of Biochemistry and Molecular Biology, Capital Medical University School of Basic Medical Sciences, Beijing, China.

phosphate (HA/TCP) group (six minipigs, two implants per minipig); (2) autologous Vc-induced periodontal ligament stem cells (PDLSCs) sheet wrapping the HA/TCP/dental pulp stem cell (DPSC) (six minipigs, two implants per minipig); (3) allogeneic Vc-induced PDLSCs sheet wrapping the HA/TCP/DPSC (six minipigs, two implants per minipig). To test the properties of the bio-root before crown restoration, three animals in each group were sacrificed at 6 months postimplantation. The rest three animals of each group were sacrificed for further analysis at 6 months post-crown restoration.

Cell culture and PDLSCs sheet

The isolation and culture of PDLSCs and DPSCs were isolated and cultured from single-colony clusters as described in previous reports [10–12]. In this study, PDLSCs were used for periodontal-like tissue regeneration and DPSCs for dentin-like tissue regeneration. Briefly, the periodontal ligament (PDL) was gently separated from the middle third root surface of the tooth, and the pulp tissue was gently separated from the crown and root. The tissues were digested in a solution of 3 mg/mL collagenase type I (Sigma-Aldrich Corp.) and 4 mg/mL dispase II (Sigma-Aldrich) for 1 h at 37°C. Single-cell suspensions were obtained by passing the cells through a 70-μm strainer (Falcon, BD Labware. To identify putative stem cells, single-cell suspensions (1×10^4–1×10^5 cells) were seeded into 10-cm culture dishes (Costar, Inc.,) with alpha-modification of the Eagle's medium (Gibco; Invitrogen Corp.) supplemented with 15% fetal bovine serum (FBS; Gibco), 2 mM glutamine, 100 U/mL penicillin, and 100 μg/mL streptomycin (Invitrogen Corp.), and then incubated at 37°C in 5% carbon dioxide. To assess colony-forming efficiency, day 10 cultures were fixed with 4% formalin, and then stained with 0.1% toluidine blue. Aggregates of 50 or more cells were scored as colonies. To examine multilineage differentiation potential of DPSCs and PDLSCs, cells were seeded onto 24-well plates (Costar) at 2.0×10^4 cells/cm^2. Subconfluent cultures were incubated in the odontogenic medium (Invitrogen Corp.) and adipogenic medium (Invitrogen Corp.) for 4 weeks. The medium was changed every 2–3 days. Calcification of the extracellular matrix (ECM) was observed with von Kossa staining. Oil red O staining was used to identify lipid-laden fat cells.

To obtain the PDLSC sheet, 1×10^5 PDLSCs (second or third passages) were subcultured in 60-mm dishes, and 20.0 μg/mL Vc (Sigma-Aldrich) was added to the culture medium for the duration of the experiment to achieve its full potential [13]. The cells became confluent after 2–3 days of culture. The confluent cells were cultured in dishes for 7–10 days until the cells on the edge of the dishes wrapped, which implied that cell sheets formed and could be detached. Samples of the PDLSCs sheet were processed for histological examination, transmission electron microscopy, and immunofluorescence, which were conducted three times.

Acridine orange and ethidium bromide staining

Living cells (green nucleus with a red-orange cytoplasm) were distinguished with acridine orange (AO) and ethidium bromide (EB; both from Sigma-Aldrich) staining. DPSCs seeded on the HA/TCP scaffold were given a combined staining of AO (50 mg/mL) and EB (5 mg/mL) for 5 min at room temperature and examined by a confocal laser scanning microscope (four-line argon primary laser/green HeNe laser; Carl Zeiss Ltd.).

Preparation of bio-root complex before implantation

The confluent DPSCs (second or third passages) were detached from the culture flask with 0.05% trypsin, centrifuged, and resuspended in a 1 mL culture medium. About 1×10^6 DPSCs were seeded onto HA/TCP scaffolds of consistent size, with the ratio between HA and TCP of 2:8 and the core diameter of 200–300 μm. After subculturing DPSCs with HA/TCP, the DPSC/HA/TCP composites were transferred into the perfusion culture container (Minucells and Minutissue). The medium flow was adjusted to a rate of 2 mL/h. The perfusion system was maintained at 37°C using a thermo plate. DPSCs were seeded on HA/TCP scaffolds and cultured in the bioreactor for 5–7 days. PDLSCs were used to prepare the Vc-induced PDLSC sheet. A PDLSC sheet was used to wrap the HA/TCP/DPSC.

Transfection of eGFP gene (green fluorescent protein labeling)

Conditional retroviral supernatants were produced by the stable retrovirus-producing cell lines PG13/eGFP as described previously [14,15]. For transfection, $\sim1\times10^6$ PDLSCs or DPSCs grown in 75-cm^2 flasks were incubated for ~20 h with a mixture of a viral supernatant and the growth medium at equal volumes and in the presence of 5 μg/mL protamine from salmon (Sigma-Aldrich). A repeated transfection was performed during a period of 72 h, and the transfected cultures were selected with 3 μg/mL puromycin dihydrochloride from *Streptomyces alboniger* (Sigma-Aldrich) for 24 h.

Bio-root implantation in swine

To simulate the clinical condition, we surgically created a tooth loss by extracting a tooth. After the extracted socket cured 3 months later, we generated a root-shaped jaw bone implant socket using a dental implant machine. Vc-induced PDLSCs sheet wrapping the HA/TCP/DPSC was implanted into the jaw bone implant socket and sutured. Six months after implantation, the implant was re-exposed and a core filled in the postchannel. A premade porcelain crown was cemented to the HA/TCP/DPSC/PDLSCs sheet structure. The porcelain crown was retained in the swine for 6 months performing normal tooth function.

Clinical and radiological evaluations

Probing depth, primary stability, gingivitis, and peri-implantitis were used to assess the clinical features of the bio-root. The primary stability was assessed manually by one blinded periodontist for triplicate times. The gingival condition was assessed by the gingival index as previously described [16]. Gingivitis radiological evaluations, including X-ray and microcomputed tomography (CT), were performed on the regenerated bio-root 6 months post-transplantation. The micro-CT scanner (Inveon CT, Siemens AG) was used to determine the changes in PDLSCs around the HA/TCP/DPSCs. Specimens were scanned with a resolution of

0.22 mm; 692 scan slices were taken and reconstructed according to the manufacturer's recommendations (Inveon CT). The output was displayed as three-dimensional (3D) stacks using Inveon Research Workplace. The thresholds used in this study were 68–1,732 Housefield Units (HU) for cortical bone and −70–67 HU for cancellous bone based on threshold calculations for samples of porcine femur bone.

Semiquantitative and histomorphometric analysis

The animals were sacrificed 6 months post-transplantation. The grafts were fixed with 4% formalin, decalcified with buffered 10% ethylenediaminetetaraceticacid (EDTA) (pH 8.0), and then embedded in paraffin. Sections (5 mm) were deparaffinized and stained with hematoxylin–eosin (HE). Six equidistantly spaced microscopic fields were analyzed by one blinded histological expert. The extent of mineralized tissues was analyzed semiquantitatively by histomorphometric techniques (Image-Pro Express).

Ultrastructure evaluation

Scanning electron microscopy (SEM) was used to examine the ultrastructure of the bioengineered root. The transplant was fixed using 2.5% glutaraldehyde in a 0.1 M sodium cacodylate buffer (pH 7.2) for 2 h at 4°C. After washing with the sodium dimethylarsenate buffer, the cells were postfixed in 1% osmium tetroxide, dehydrated with gradient alcohol, and incubated with isoamyl acetate. After gold coating, the samples were examined using a Hitachi S-520 scanning electron microscope (Hitachi).

Mechanical properties of the regenerated root

Compressive strength was tested by a H5KS type force test system with 1 mm/min loading (Tinius Olsen H5KS testing machine, Tinius Olsen, Ltd.). A newly formed bio-root was harvested 6 months after transplantation and divided into three pieces. The compressive strength of each piece was measured separately. The compressive strength of the natural minipig roots and original HA/TCP carriers were also measured ($n = 5$).

Immunohistochemistry of cultured cells, harvested PDLSC sheets, and regenerated bio-root tissues

DPSCs and PDLSCs were subcultured in 24-chamber slides. Cells were fixed in 4% paraformaldehyde for 15 min and blocked with phosphate-buffered saline (PBS) containing 10% normal equine serum at room temperature for 45 min. Then, cells were incubated with diluted anti-STRO-1 (STRO-1, 1:200; Invitrogen) and anti-CD146 (CD146, 1:500; Sigma-Aldrich) overnight at 4°C, washed with PBS, and then incubated with fluorescein isothiocyanate (FITC)-conjugated or phycoerythrin (PE)-conjugated second antibodies at room temperature in the dark for 45 min, and 4′,6-diamidino-2-phenylindole staining in the dark for 5 min. After washing with PBS, the slides were mounted, and then analyzed using a fluorescence microscope.

Cryosections (12-μm thick) of harvested PDLSC sheets were treated with 5% bovine serum albumin (BSA) in 50 mM Tris-buffered saline (TBS, pH 7.2) containing 0.4% Triton X-100 for 60 min at room temperature. Sections were then incubated overnight at 4°C with primary antibodies diluted with 1% BSA in TBS containing 0.4% Triton X-100. Primary antibodies included anti-vimentin (vimentin, 1:500; Sigma-Aldrich), anti-fibronectin (1:500; Sigma-Aldrich) and anti-collagen type I (COLI, 1:1,000; Sigma-Aldrich). Immunoreactivity was detected using PE-labeled goat anti-rabbit immunoglobulin G (IgG, 1:200; Chemicon) or FITC-labeled goat anti-mouse IgG (1:200; Chemicon). Stained cells were observed using confocal laser scanning microscopy (four-line argon primary laser/green HeNe laser; Carl Zeiss Ltd.).

The regenerated bio-root tissues were removed and immersed in 4% paraformaldehyde in PBS. After fixation, the tissues were decalcified in 4.5% EDTA (pH 7.4) at 4°C. For immunohistochemistry, the primary antibodies anti-dentin sialoprotein (1:200; LF-151), anti-COLI (1:1,000; Sigma-Aldrich), and anti-von Willibrand factor (αvWF pAb, 1:100; Chemicon) were used. Immunoreactivity was detected using fluorescence-conjugated goat anti-rabbit IgG (1:200; Chemicon). The sections were observed using an Axio Imager A1 (Carl Zeiss) with an AxioCAM MRc5 (Zeiss) and processed with AxioVision software (Zeiss). Fluorescent images were acquired using an Axiovert 200M (Carl Zeiss) with an AxioCAM MRm (Zeiss).

Flow cytometric analysis

To examine stem cell surface molecule expression in DPSCs and PDLSCs, 2.5×10^5 third passage cells in 1.5 mL eppendorf tubes were fixed with 4% paraformaldehyde for 15 min. Primary STRO-1 and CD146 antibodies were added into the tubes and incubated at room temperature for 1 h followed by FITC-conjugated or PE-conjugated second antibodies at room temperature in the dark for 45 min. The percentage of positive staining cells to STRO-1 and CD146 were assessed using a fluorescence-activated cell sorting Calibur flow cytometry (Becton Dickinson Immunocytometry Systems).

To evaluate systemic immunological parameters, blood (75 μL) was collected into 1 mL PBS containing 5 μM EDTA (10 μM of 0.5 M stock) and mixed immediately to prevent clotting. Tubes were kept on ice. RBCs were lysed using the Gey's solution. Cells were washed two to three times with the FACS buffer (PBS supplemented with either 1% BSA or 5% FBS and containing 0.05% NaN_3). The pellet was suspended from the final wash in a 50 μL FACS buffer. PE/Cy5-conjugated CD3, FITC-conjugated CD4, and PE-conjugated CD8 antibodies (Abcam Ltd.) were added to cell suspension and mixed gently. Fluorescence was analyzed by a FACSCalibur flow cytometer with CellQuest software (BD Bioscience).

Statistical analysis

Statistical significance was assessed by the two-tailed Student's *t*-test or analysis of variance (post hoc test: SNK-q test, if necessary), a *P*-value less than 0.05 was considered statistically significant.

Results

Stem cell properties of DPSCs and PDLSCs from miniature pig

We developed a strategy for bio-root regeneration (Supplementary Fig. S1; Supplementary Data are available online

at www.liebertpub.com/scd). Stem cell properties of DPSCs and PDLSCs were examined. The ability of DPSCs and PDLSCs to form adherent clonogenic cell clusters was shown by the formation of $48 \pm 11/10^4$ and $57 \pm 11/10^4$ colonies, respectively (Supplementary Fig. S2A–C). Both DPSCs and PDLSCs were positive for STRO-1 and CD146 staining (Supplementary Fig. S2D–K). After 4 weeks culture with the odontogenic-inductive medium, both DPSCs and PDLSCs produced a dense ECM. DPSCs and PDLSCs odontogenic differentiation was characterized by the formation of mineralized nodules as assessed by von Kossa staining, indicating calcium accumulation in vitro (Supplementary Fig. S2L, M). DPSCs and PDLSCs were able to develop into oil red O-positive lipid-laden fat cells following 4 weeks of culture in an adipogenic-inductive medium (Supplementary Fig. S2N, O).

Characteristics of DPSCs seeded on HA/TCP scaffold and harvested PDLSC sheet

To create a 3D root shape scaffold before transplantation, HA/TCP/DPSCs were cultured for 5–7 days in a bioreactor. SEM images of the top surface and cross section revealed that the DPSCs were actually present at a high density in the HA/TCP (Fig. 1A–D). AO and EB staining showed that there was a dense cell population within the scaffolds and most of them were living cells. (Fig. 1E, F). To prepare the PDLSC sheet to cover the DPSC scaffold, PDLSCs were treated with 20 μg/mL of the Vc medium for 10–13 days and a complete PDLSCs sheet formed (Fig. 1G). HE staining showed that the collected whole PDLSCs sheet had two or three layers and uniformly spread as a two-dimensional tissue structure (Fig. 1H). Immunostaining for vimentin was positive, indicating the features of MSCs (Fig. 1I). Fibronectin and type I collagen, main components of the ECM, were present in the harvested PDLSC sheet, showing preservation of the ECM in the PDLSC sheet (Fig. 1J, K).

Analysis of the bio-root 6 months after implantation

Six months after transplantation, bone-like tissue formation was observed in the HA/TCP group (Fig. 2A), and no obvious boundary was present between the newly regenerated tissue and bone in X-ray (Fig. 2B). The HA/TCP/DPSC/PDLSC sheet implant formed a hard root structure (Fig. 2C), and a clear PDL space was found between the implant and surrounding bony tissue in X-ray (Fig. 2D). Micro-CT demonstrated that there was no obvious hard root structure and PDL space in the HA/TCP group (Fig. 2E, F), whereas a visible root structure and PDL space-like areas in the HA/TCP/DPSC/PDLSC sheet group (Fig. 2G, H). HE staining showed bone formation and HA/TCP particles were left in the HA/TCP group (Fig. 2I). In autologous and allogeneic HA/TCP/DPSC/PDLSC sheet transplants, PDL-like tissue was generated along a dentin-like matrix structure (Fig. 2J, K). Semiquantitative analysis showed that the mineralized tissue regeneration capacity of autologous or allogeneic groups was significantly higher compared with the HA/TCP group before crown restoration. Percentage of mineralized tissues at 6 months after crown restoration was significantly higher than that before crown restoration in

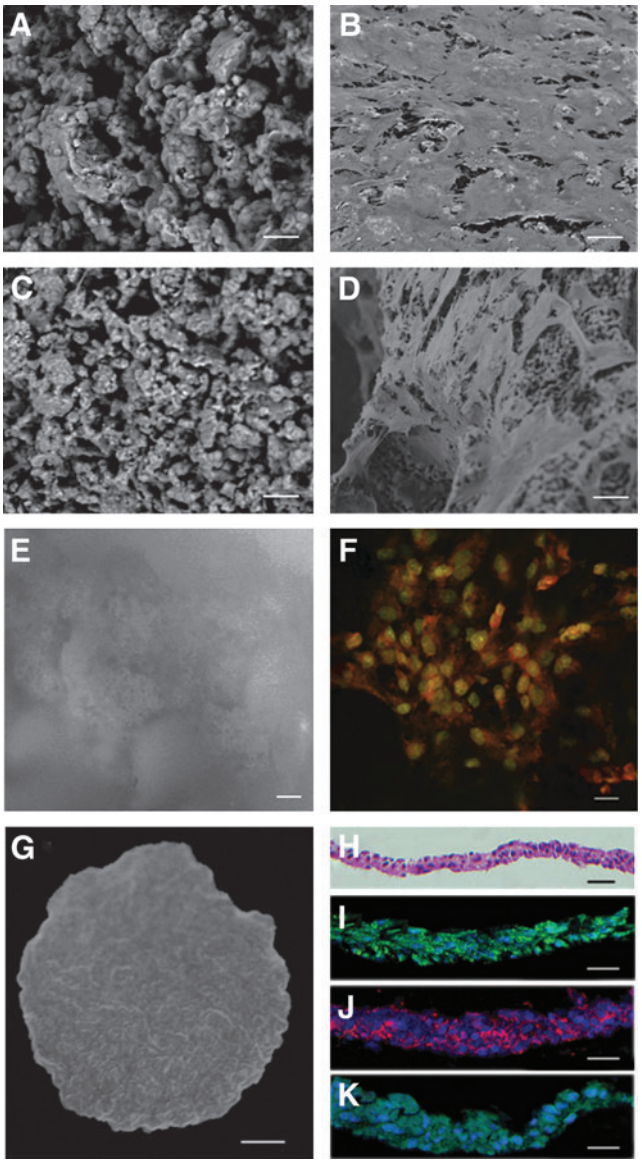

FIG. 1. Morphological validation of dental pulp stem cells (DPSCs) seeded on the hydroxyapatite tricalcium phosphate (HA/TCP) scaffold and engineered periodontal ligament stem cell (PDLSC) sheet. **(A)** Scanning electron microscopy (SEM) of the top surface of the nude HA/TCP scaffold without cell transplantation. **(B)** SEM images of the top surface of DPSCs seeded on scaffolds showed that DPSCs were present at a high density at the surface. **(C)** SEM of the cross section of the nude HA/TCP scaffold. **(D)** SEM images of a cross section of the scaffolds revealed that DPSCs were also present at a high density in the scaffolds. **(E)** Acridine orange and ethidium bromide (AO/EB) staining of HA/TCP staining. **(F)** AO/EB staining of DPSCs seeded on scaffolds showed that the cells were alive. **(G)** Gross appearance of the Vc-induced PDLSCs sheet. **(H)** Histological analyses of the harvested sheets by hematoxylin–eosin (HE) staining. **(I–K)** Immunofluorescence of vimentin, fibronectin immunofluorescence, and type I collagen showing the PDLSC sheet preserved the extracellular matrix (ECM). Scale bar: **(A–F)**, **(H–K)** 20 μm; **(G)** 0.25 cm.

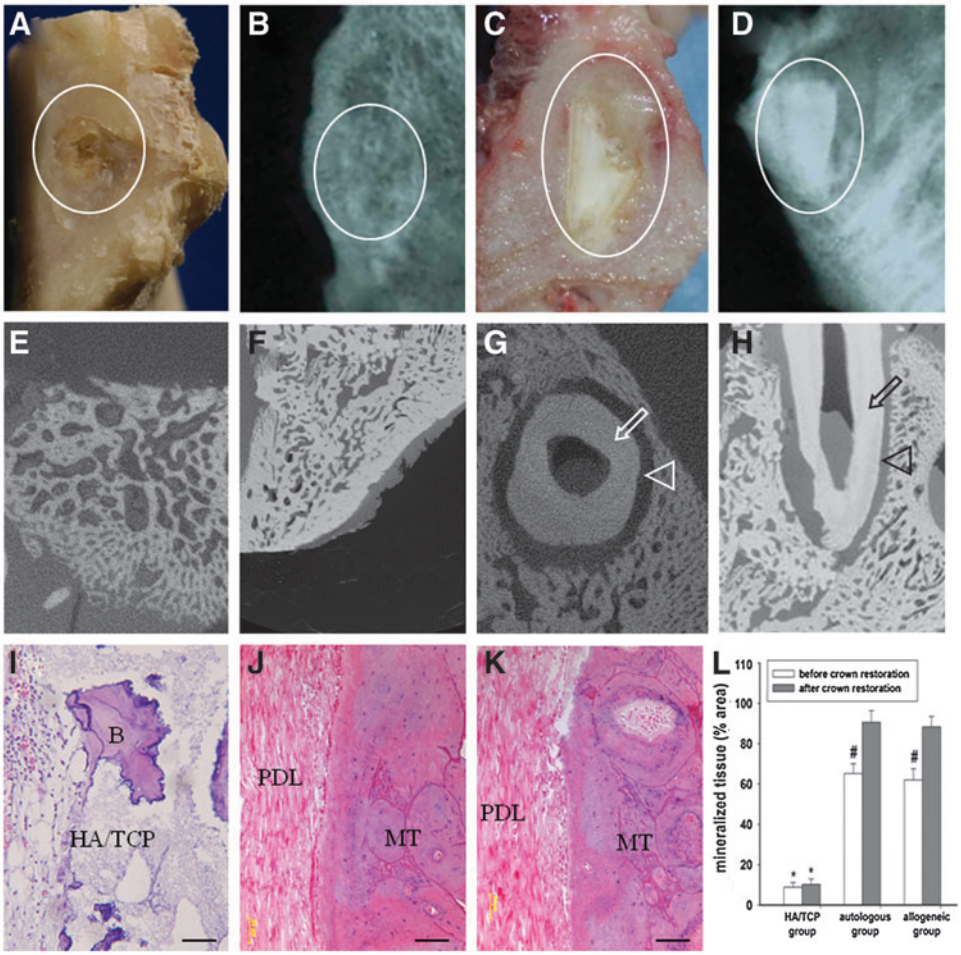

FIG. 2. Gross, radiographic, and histological analysis of the bio-root 6 months after transplantation. **(A, C)** Gross view of the general shape of HA/TCP and the bio-root 6 months after transplantation (ellipse). **(B, D)** X-rays revealed that HA/TCP formed tissues without an obvious dental structure (ellipses), but the HA/TCP/DPSC/PDLSC sheet implant formed a hard root structure (ellipses). **(E, F)** No obvious boundary was observed between newly regenerated tissue and bone in the microcomputed tomography scan image of the HA/TCP group. **(G, H)** A hard root structure (*arrows*) was present and a clear PDL space found between the implant and surrounding bony tissue (*triangle arrows*). **(I–K)** HE staining showed some bone formation and HA/TCP remaining in the HA/TCP group **(I)**, and PDL-like tissues were generated parallel to the dentin-like matrix structure in the autologous group **(J)** and allogeneic group **(K)**. **(L)** Semiquantitative analysis showed that mineralized tissue regeneration capacity of autologous or allogeneic groups was significantly higher compared with the HA/TCP group. Percentage of mineralized tissues at 6 months after crown restoration was significantly higher than that before crown restoration in both autologous and allogeneic groups. No significant difference of regenerated mineralized tissue percentages was found between autologous and allogeneic groups. Scale bar: **(I–K)** 200 μm. B, bone; HA/TCP, hydroxyapatite/tricalcium phosphate; PDL, periodontal ligament; MT, mineralized tissue. $^{*}P < 0.01$ compared with autologous or allogeneic groups; $^{\#}P < 0.01$ compared with autologous or allogeneic groups after crown restoration.

both autologous and allogeneic groups. There were no significant differences between autologous and allogeneic groups before crown restoration (Fig. 2L).

Analysis of the bio-root 6 months after crown restoration

To test the function of the newly regenerated bio-root, a premade porcelain crown was cemented to the HA/TCP/DPSC/PDLSC sheet implant (Fig. 3A, B) and retained for 6 months (Fig. 3C). We assessed the response of the bio-root subjected to tooth function for 6 months. The percentage of mineralized tissues at 6 months after crown restoration was significantly higher than that before crown restoration in both autologous and allogeneic groups (Fig. 2L). The regenerated bio-roots in autologous and allogeneic groups demonstrated a significantly improved compressive strength compared to the original HA/TCP carriers, almost close to a normal tooth (Fig. 3D), while only bone formation and HA/TCP particles remained in the HA/TCP group (Fig. 3E). PDL-like tissue became slanting and regular from paralleled to dentin-like structure, which indicating that PDL-like tissue became the functional periodontium in autologous (Fig. 3F) and allogeneic groups (Fig. 3G) like a normal root (Fig. 3H). Semiquantitative analysis showed that mineralized tissues markedly increased 6 months after crown restoration, autologous (Fig. 3J) and allogeneic transplants (Fig. 3K) were capable of forming dentinal tubule-like structures with few

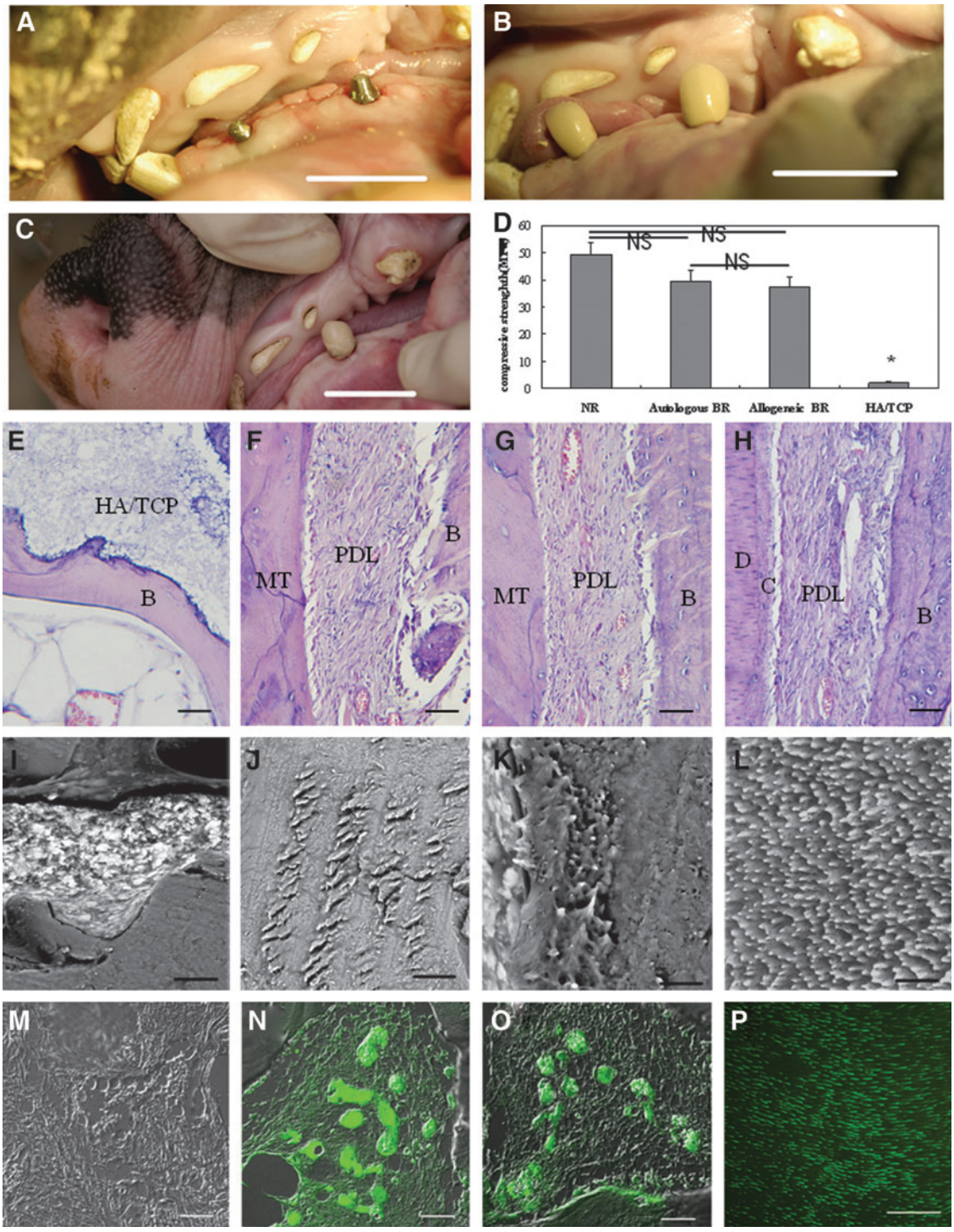

FIG. 3. Structural changes and compressive strength of the bio-root 6 months after crown restoration. **(A)** Six months after implantation, the implant was re-exposed and a core filled in the postchannel. **(B)** A premade porcelain crown was cemented to the HA/TCP/DPSC/PDLSC structure. The normal occlusion was established after crown restoration for functional performance. **(C)** The porcelain crown was retained for 6 months for normal functional performance. **(D)** The compressive strength of regenerated bio-roots in the autologous and allogeneic groups was close to normal teeth, significantly higher compared with original HA/TCP carriers ($n = 5$). **(E–H)** HE staining showed that PDL-like tissue became slanting and regular from parallel to the dentin-like structure in the autologous group **(F)** and allogeneic group **(G)** compared to the normal root **(H)**. Only bone formation and HA/TCP particles remained in the HA/TCP group **(E)**. Ultrastructural analysis of the dentin-like structure revealed that many HA/TCP particles remained and no dentinal tubule-like structure formation was seen in the HA/TCP group **(I)**. A dentinal tubule-like structure with few HA/TCP particles remaining was found in the autologous group **(J)** and allogeneic group **(K)**, similar to the normal root **(L)**. The HA/TCP group was negative for the dentin sialophosphoprotein (DSPP) **(M)**. The dentin-like structure was positive for the DSPP in the autologous group **(N)** and allogeneic group **(O)**, similar to the normal root **(P)**. **(L–P)** cross section. Scale bar: **(A–C)** 2 cm; **(E–H)** 200 μm; **(I–L)** 6 μm; **(M–P)** 40 μm. B, bone; D, dentin; C, cementum; NS, no significance. *$P < 0.05$, compared with other groups.

remaining HA/TCP particles like normal tooth (Fig. 3L). Most importantly, the dentin sialophosphoprotein (DSPP) was not observed in the HA/TCP group (Fig. 3M), but found in both autologous (Fig. 3N) and allogeneic (Fig. 3O) transplants, and the structure of which was similar to the normal root (Fig. 3P). These data demonstrated that structural and functional bio-root regeneration was successfully achieved in the minipig model.

Structural analysis of the bio-root PDL before and after crown restoration

We tested the regenerated PDL structure before and after crown restoration in autologous and allogeneic HA/TCP/DPSC/PDLSC sheet groups (Fig. 4). PDL paralleled mineralized tissue and was positive for COLI and vWF before crown restoration (Fig. 4A, G, J). After crown restoration, PDL was inserted to mineralized tissue and positive for COLI and vWF (Fig. 4B, H, K), which is similar to the normal root (Fig. 4C, I, L). Polarized light indicated there was no typical Sharpey's-fiber-like tissue formation within the PDL before crown restoration (Fig. 4D), but there was a Sharpey's-fiber-like tissue formation within the PDL after crown restoration (Fig. 4E), typical Sharpey's fibers in the normal tooth (Fig. 4F). These findings indicated that bio-root structures gradually adjusted after the functional performance of the crown restoration.

Green fluorescent protein labeling of pretransplantation and post-transplantation

PDLSCs and DPSCs were positive for the green fluorescent protein (GFP) with transfection efficiency of 94%–96% (Fig. 5A–D). After seeded on the HA/TCP scaffold, GFP-positive DPSCs were present within scaffold pretransplantation (Fig. 5E). GFP-positive cells were absent in the HA/TCP group (Fig. 5F), and were present 1 month after transplantation in autologous (Fig. 5G) and allogeneic groups (Fig. 5H), indicating that bio-root tissue regeneration was mediated by transplanted stem cells.

Clinical assessment and evaluation of systemic immunological parameters after bio-root implantation

Six months after crown restoration, the clinical features of the bio-root, including probing depth, gingival recession, and attachment loss, were comparable with normal minipig teeth. No significant differences in these clinical evaluations were observed between bio-root teeth and normal teeth (Fig. 6, $n=5$, $P>0.05$). No difference of primary stability was found between both bio-root teeth and normal teeth. No gingivitis or peri-implantitis was found in bio-root teeth. These findings indicate that allogeneic stem cell-based functional bio-roots regenerated well in the swine model.

To test the immunological reaction after allogeneic DPSC/PDLSs sheet transplantation, we analyzed T cell-related immunological markers (Fig. 7), routine blood and biochemical tests, and immunoglobulin tests (data not shown) in whole blood. We found no significant differences between allogeneic and autologous groups based on this analysis, suggesting that there were no immunological rejections in the animals that received allogeneic DPSC/PDLSC sheet transplantation.

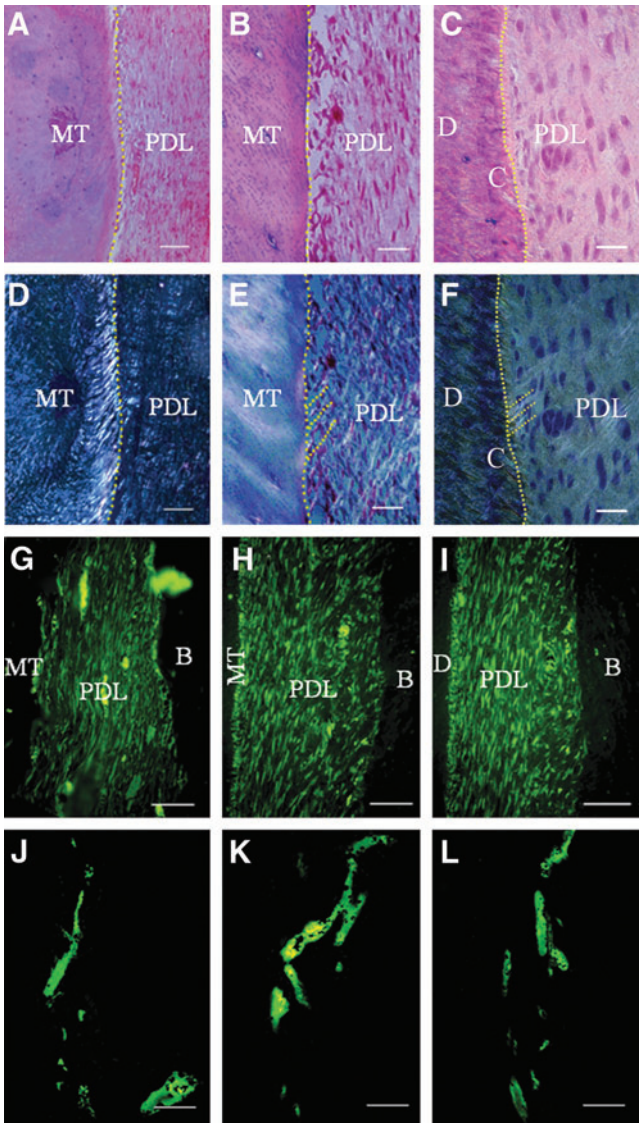

FIG. 4. Structural analysis of the bio-root PDL before and after crown restoration. **(A, D, G, J)** Bio-root PDL before crown restoration. **(B, E, H, K)** Bio-root PDL after crown restoration. **(C, F, I, L)** Normal tooth PDL. **(E, F)** Polarized light indicated there was no typical Sharpey's fiber-like tissue formation within the PDL before crown restoration **(D)**, but there was Sharpey's fiber-like tissue formation within the PDL after crown restoration **(E)**, typical Sharpey's fibers in normal tooth (*dashed stripes*) **(F)**. PDL was parallel to MT **(A)** and positive for COLI **(G)** and von Willibrand factor (vWF) **(J)** before crown restoration. PDL was inserted to mineralized tissue **(B)** and positive for COLI **(H)** and vWF **(K)** after crown restoration, similar to the normal tooth root **(C, I, L)**. Scale bar: **(A–F)** 100 μm; **(G–L)** 20 μm.

Discussion

In the present study, we generated tooth loss for 3 months and used a dental planter to create an implant socket to mimic clinical conditions. Vc-induced PDLSC sheets, with preserved cellular junctions, ECM, and mimicked cellular

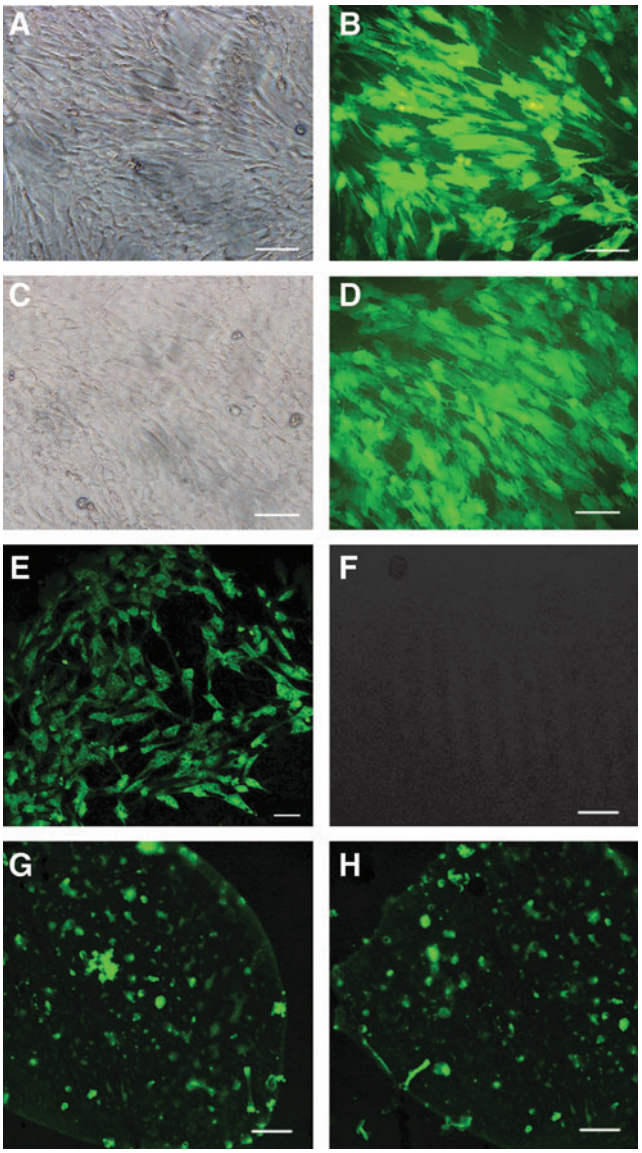

FIG. 5. Green fluorescent protein (GFP)-labeled cells before and after transplantation. PDLSCs **(A, B)** and DPSCs **(C, D)** were positive for GFP after transfection. **(E)** GFP-positive DPSCs were present within the HA/TCP scaffold pre-transplantation. **(F–H)** GFP-positive cells were present 1 month after transplantation in the autologous **(G)** and allogeneic groups **(H)**, and negative GFP cells were found in the HA/TCP group **(F)**. Scale bar: **(A–E)** 50 μm; **(F–H)** 100 μm.

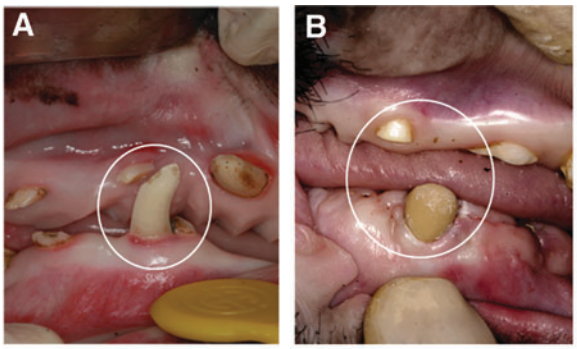

Follow up

Measurement	Normal teeth	Bio-root teeth
Probing depth (mm)	2.4±0.5	2.6±0.4
Primary stability	–	–
Gingivitis	–	–
Peri-implantitis	–	–

FIG. 6. Clinical assessment and evaluation of systemic immunological parameters after bio-root implantation. A porcelain crown was restored 6 months after bio-root implantation. **(A, B)** Clinical functional assessments and follow-up observations were made for both normal tooth **(A)** and bio-root **(B)** after crown restoration. No significant differences in probing depth (PD) were observed between bio-root teeth and normal teeth ($n=5$, $P>0.05$). Biological primary stability was found in both the bio-root teeth and normal teeth. No gingivitis or peri-implantitis were found in bio-root teeth. "–" in primary stability: no primary stability. Peri-implantitis: inflammation of peri-implant tissues such as swelling, bleeding.

microenvironments, were used. Six months after implantation, to obtain the functional performance of a regenerated bio-root, the regenerated bio-root was subjected to normal tooth function for another 6 months. The bio-root was found to have the characteristics of a normal tooth, including the dentinal tubule-like structure and the functional PDL-like structure. Interestingly, positive massive DSPP staining was found in regenerated bio-root tissues, indicating allogeneic DPSC-mediated dentin regeneration.

MSCs are multipotent progenitor cells that have emerged as a promising tool for clinical application, which are found in the bone marrow [17], adipose tissue [18], cord blood [19], and dental tissues [10,11]. The low immunogenicity and immunomodulation function of MSCs are used for allogeneic application [7,20,21]. Previous vitro studies have suggested that MSCs could exert a potent immunosuppressive effect in vitro [22,23]. In line with their immunosuppressive capacities in vitro, MSCs also display immunosuppressive capacities in vivo; allogeneic MSCs may prolong skin allograft survival in immunocompetent baboons [22]. However, other studies indicate that MSCs are not intrinsically immunoprivileged and are capable of inducing a memory T-cell response after injection in vivo in immunocompetent hosts [24] and yielded no clinical benefit on the incidence or severity of graft-versus-host disease (GVHD) [23]. Although conflicting results have been reported, further clinical interest has been raised by the observation that allogeneic MSCs conferred significant therapeutic effects [7,8]. The patients with acute GVHD responded to treatment with MSCs, although little is known about mechanisms of suppression of GVHD by MSCs [21]. These properties and clinical trials might open attractive possibilities to use allogeneic MSCs for different therapeutic applications.

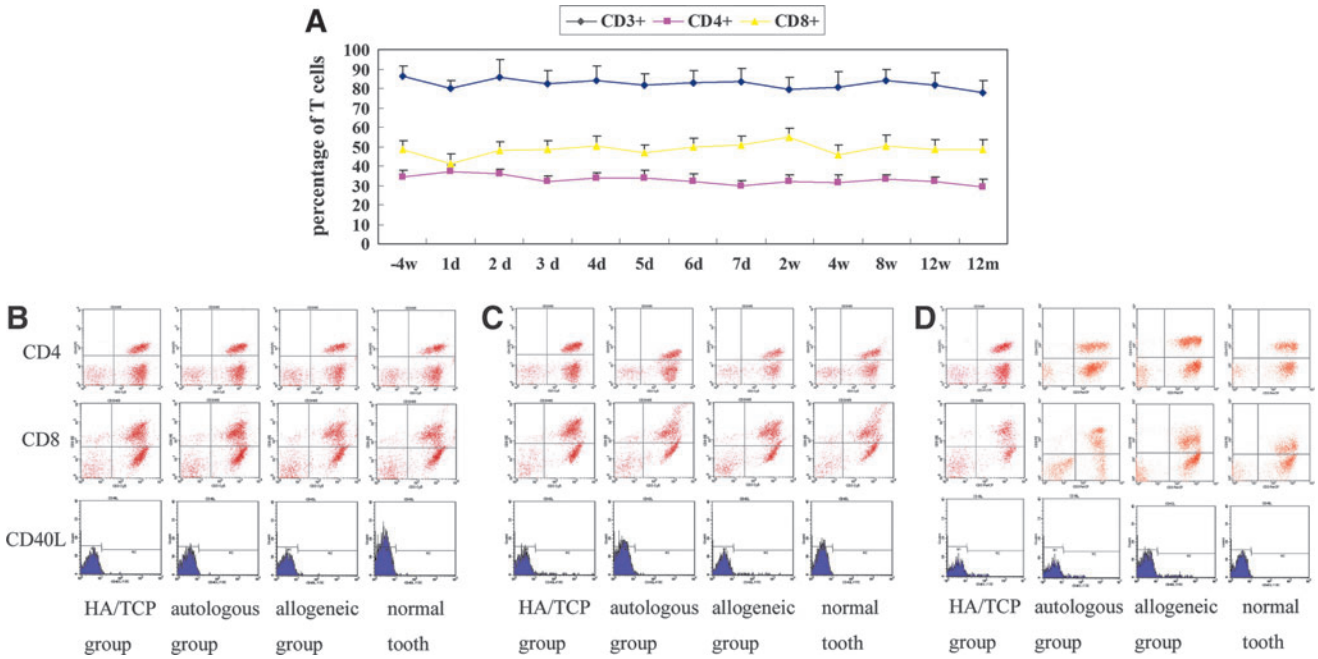

FIG. 7. Evaluation of systemic immunological parameters after bio-root implantation. **(A)** No significant differences were observed at the indicated time points regarding the percentage of $CD3^+$, $CD4^+$, and $CD8^+$ T cells in the allogeneic transplantation group ($n=3$). **(B)** The expression of $CD4^+$ and $CD8^+$ T cells, as well as CD40L, a marker of activated T cells, were nearly identical among the four test groups 3 days post-transplantation ($n=3$). **(C, D)** The percentage of $CD4^+$ and $CD8^+$ T cells and the expression of CD40L were also nearly identical among the four groups ($n=3$) 12 weeks and 12 months after transplantation.

In our previous study, we used autologous stem cells from root apical papilla (SCAP) to regenerate the bio-root. Autologous SCAP are limited in aged patients, which significantly impede their application [25]. Recent studies have shown that SCAP and DPSCs may reflect the relative developmental ages of dental stem cells and not the actual differentiation capabilities [26]. DPSCs can also regenerate a dentin-like structure like SCAP, and are easily accessible in dental clinical practice. Both DPSCs and PDLSCs are derived from mesenchymal tissue like bone marrow mesenchymal stem cells (BMMSCs), which show low immunogenicity and immunomodulation functions [7]. Similar to BMMSCs, dental MSCs, including PDLSCs, DPSCs, and SCAP possess immunomodulatory effects in vitro [27,28]. Furthermore, we previously established a novel approach for using allogeneic PDLSCs to cure periodontitis in a minipig model of periodontitis in vivo [9]. Our previous studies showed that PGE2 secreted from allogeneic PDLSCs plays a crucial role in PDLSC-mediated immunomodulation and periodontal tissue regeneration [9]. Based on these in vitro and in vivo studies, we tested the allogeneic DPSC/PDLSC sheet for bio-root regeneration and found that PDL-like tissue was generated along a dentin-like matrix structure in the autologous and allogeneic groups. T cell-related immunological markers in whole blood suggested the absence of immunological rejection in the animals. We previously explored the potential for regenerating bio-root in a newly extracted incisor socket in swine [5]. However, detailed structural and functional investigations of the bio-root are essential before application. The ECM, including COLI, integrin β1, and fibronectin is responsible for transmitting a wealth of chemical and mechanical signals that mediate key aspects of cellular physiology and determine tissue structure and function [29]. The Vc-induced PDLSC sheet created a suitable matrix for bio-root regeneration. The hard tissues of the bio-root became mature and PDL-like tissue became slanting and regular from paralleled to the dentin-like structure, indicating that functional modification occurred after crown restoration. These results suggest that the mechanical force was essential for the reconstruction of regenerated bio-root tissues as reported previously [30].

GFP-positive cells in the bio-root 1 month after transplantation indicated that exogenous cells existed in new formed tissue. Since odontoblasts, osteoblasts, cementoblasts, bone cells, and pulp cells were similar in morphology, it was hard to distinguish them at this stage. It was thought that implanted PDLSCs and DPSCs not only effected new tissue formation through direct participation in the regeneration process and eventual incorporation into regenerated tissue [31,32], but also modulated the host environment through indirect mechanisms, leading to new tissue formation, rather than through direct participation and incorporation into tissue [33–35]. Allogeneic engraftment of mouse MSCs has shown improvement in wound closure, but it is difficult to delineate the contributions of the host and the exogenous cells [36,37]. Although the endogenous cell behavior is unclear, the regenerative capacity of the endogenous cell appears minimal without exogenous engraftment or stimulation [38]. Furthermore, it is also unknown whether the host responds by recruiting existing cells or generating new cells in response to implanted PDLSCs and DPSCs.

In summary, the results demonstrated that allogeneic dental MSC-mediated bio-root regeneration is a practical approach for restoring adult tooth function in preclinical animal models and suggest a great potential for biological and functional tooth regeneration in humans.

Acknowledgments

This work was supported by Beijing Municipal Committee for Science and Technology no. Z121100005212004; National Basic Research Program of China no. 2010CB94480; Beijing Municipality no. PHR20090510, PXM 2009-014226-074691, and PXM2011-014226-07-000066; the National Institute of Dental and Craniofacial Research, National Institutes of Health, Department of Health and Human Services no. R01DE017449.

Author Disclosure Statement

The authors declare no competing financial interests.

References

1. Atala A, SB Bauer, S Soker, JJ Yoo and AB Retik. (2006). Tissue-engineered autologous bladders for patients needing cystoplasty. Lancet 367:1241–1246.
2. Zaky SH and R Cancedda. (2009). Engineering craniofacial structures: facing the challenge. J Dent Res 88:1077–1091.
3. Ikeda E, R Morita, K Nakao, K Ishida, T Nakamura, T Takano Yamamoto, M Ogawa, M Mizuno, S Kasugai and T Tsuji. (2009). Fully functional bioengineered tooth replacement as an organ replacement therapy. Proc Natl Acad Sci U S A 106:13475–13480.
4. Eckert SE, YG Choi, AR Sánchez and S Koka. (2005). Comparison of dental implant systems: quality of clinical evidence and prediction of 5-year survival. Int J Oral Maxillofac Implants 20:406–415.
5. Sonoyama W, Y Liu, D Fang, T Yamaza, BM Seo, C Zhang, H Liu, S Gronthos, CY Wang, S Wang and S Shi. (2006). Mesenchymal stem cell-mediated functional tooth regeneration in swine. PLoS One 1:e79–e92.
6. Wang S, Y Liu, D Fang and S Shi. (2007). The miniature pig: a useful large animal model for dental and orofacial research. Oral Dis 13:530–537.
7. Sun L, K Akiyama, H Zhang, T Yamaza, Y Hou, S Zhao, T Xu, A Le and S Shi. (2009). Mesenchymal stem cell transplantation reverses multiorgan dysfunction in systemic lupus erythematosus mice and humans. Stem Cells 27: 1421–1432.
8. Xu J, D Wang, D Liu, Z Fan, H Zhang, O Liu, G Ding, R Gao, C Zhang, et al. (2012). Allogeneic mesenchymal stem cell treatment alleviates experimental and clinical Sjogren's syndrome. Blood 120:3142–3151.
9. Ding G, Y Liu, W Wang, F Wei, D Liu, Z Fan, Y An, C Zhang and S Wang. (2010). Allogeneic periodontal ligament stem cell therapy for periodontitis in swine. Stem Cells 28:1829–1838.
10. Gronthos S, M Mankani, J Brahim, PG Robey and S Shi. (2000). Postnatal human dental pulp stem cells (DPSCs) *in vitro* and *in vivo*. Proc Natl Acad Sci U S A 97:13625–13630.
11. Liu Y, Y Zheng, G Ding, D Fang, C Zhang, PM Bartold, S Gronthos, S Shi and S Wang. (2008). Periodontal ligament stem cell-mediated treatment for periodontitis in miniature swine. Stem Cells 26:1065–1073.
12. Seo BM, M Miura, S Gronthos, PM Bartold, S Batouli, J Brahim, M Young, PG Robey, CY Wang and S Shi. (2004). Investigation of multipotent postnatal stem cells from human periodontal ligament. Lancet 364:149–155.
13. Wei F, C Qu, T Song, G Ding, Z Fan, D Liu, Y Liu, C Zhang, S Shi and S Wang. (2012). Vitamin C treatment promotes mesenchymal stem cell sheet formation and tissue regeneration by elevating telomerase activity. J Cell Physiol 227:3216–3224.
14. Brazelton TR and HM Blau. (2005). Optimizing techniques for tracking transplanted stem cells *in vivo*. Stem Cells 23:1251–1265.
15. Zhang H, Y Zhao, C Zhao, S Yu, D Duan and Q Xu. (2005). Long-term expansion of human neural progenitor cells by epigenetic stimulation *in vitro*. Neurosci Res 51:157–165.
16. Silness J and H Löe. (1964). Periodontal disease in pregnancy II. Correlation between oral hygiene and periodontal condition. Acta Odontol Scand 22:121–135.
17. Campagnoli C, IA Roberts, S Kumar, PR Bennett, I Bellantuono and NM Fisk. (2001). Identification of mesenchymal stem/progenitor cells in human first- trimester fetal blood, liver, and bone marrow. Blood 98:2396–2402.
18. Zuk PA, M Zhu, P Ashjian, DA De Ugarte, JI Huang, H Mizuno, ZC Alfonso, JK Fraser, P Benhaim and MH Hedrick. (2002). Human adipose tissue is a source of multipotent stem cells. Mol Biol Cell 13:4279–4295.
19. Erices A, P Conget and JJ Minguell. (2000). Mesenchymal progenitor cells in human umbilical cord blood. Br J Haematol 109:235–242.
20. Gonzalez Rey E, P Anderson, MA González, L Rico, D Büscher and M Delgado. (2009). Human adult stem cells derived from adipose tissue protect against experimental colitis and sepsis. Gut 58:929–939.
21. Le Blanc K, F Frassoni, L Ball, F Locatelli, H Roelofs, I Lewis, E Lanino, B Sundberg, ME Bernardo, et al. (2008). Mesenchymal stem cells for treatment of steroid-resistant, severe, acute graft-versus-host disease: a phase II study. Lancet 371: 1579–1586.
22. Bartholomew A, C Sturgeon, M Siatskas, K Ferrer, K McIntosh, S Patil, W Hardy, S Devine, D Ucker, et al. (2002). Mesenchymal stem cells suppress lymphocyte proliferation *in vitro* and prolong skin graft survival *in vivo*. Exp Hematol 30:42–48.
23. Sudres M, F Norol, A Trenado, S Grégoire, F Charlotte, B Levacher, JJ Lataillade, P Bourin, X Holy, et al. (2006). Bone marrow mesenchymal stem cells suppress lymphocyte proliferation *in vitro* but fail to prevent graft-versus-host disease in mice. J Immunol 176:7761–7767.
24. Nauta AJ, G Westerhuis, AB Kruisselbrink, EG Lurvink, R Willemze and WE Fibbe. (2006). Donor-derived mesenchymal stem cells are immunogenic in an allogeneic host and stimulate donor graft rejection in a nonmyeloablative setting. Blood 108:2114–2120.
25. Sonoyama W, Y Liu, T Yamaza, RS Tuan, S Wang, S Shi and GT Huang. (2008). Characterization of the apical papilla and its residing stem cells from human immature permanent teeth: a pilot study. J Endod 34:166–171.
26. Bakopoulou A, G Leyhausen, J Volk, A Tsiftsoglou, P Garefis, P Koidis and W Geurtsen. (2011). Comparative analysis of *in vitro* osteo/odontogenic differentiation potential of human dental pulp stem cells (DPSCs) and stem cells from the apical papilla (SCAP). Arch Oral Biol 56:709–721.
27. Ding G, Y Liu, Y An, C Zhang, S Shi, W Wang and S Wang. (2010). Suppression of T cell proliferation by root apical papilla stem cells *in vitro*. Cells Tissues Organs 191:357–364.

28. Wada N, D Menicanin, S Shi, PM Bartold and S Gronthos. (2009). Immunomodulatory properties of human periodontal ligament stem cells. J Cell Physiol 219:667–676.
29. Nelson CM and MJ Bissell. (2006). Of extracellular matrix, scaffolds, and signaling: tissue architecture regulates development, homeostasis, and cancer. Annu Rev Cell Dev Biol 22: 287–309.
30. Boerckel JD, KM Dupont, YM Kolambkar, AS Lin and RE Guldberg. (2009). *In vivo* model for evaluating the effects of mechanical stimulation on tissue-engineered bone repair. J. Biomech Eng 131:084502.
31. Wu Y, L Chen, PG Scott and EE Tredget. (2007). Mesenchymal stem cells enhance wound healing through differentiation and angiogenesis. Stem Cells 25:2648–2659.
32. Prockop DJ, CA Gregory and JL Spees. (2003). One strategy for cell and gene therapy: harnessing the power of adult stem cells to repair tissues. Proc Natl Acad Sci U S A 100 (suppl 1):11917–11923.
33. Javazon EH, SG Keswani, AT Badillo, TM Crombleholme, PW Zoltick, AP Radu, ED Kozin, K Beggs, AA Malik and AW Flake. Enhanced epithelial gap closure and increased angiogenesis in wounds of diabetic mice treated with adult murine bone marrow stromal progenitor cells. Wound Repair Regen 15:350–359.
34. Daley GQ and DT Scadden. (2008). Prospects for stem cell-based therapy. Cell 132:544–548.
35. Jackson WM, LJ Nesti and RS Tuan. (2012). Mesenchymal stem cell therapy for attenuation of scar formation during wound healing. Stem Cell Res Ther 3:20.
36. Shin L and DA Peterson. (2012). Impaired therapeutic capacity of autologous stem cells in a model of type 2 diabetes. Stem Cells Transl Med 1:125–135.
37. Badillo AT, RA Redden, L Zhang, EJ Doolin and KW Liechty. (2007). Treatment of diabetic wounds with fetal murine mesenchymal stromal cells enhances wound closure. Cell Tissue Res 329:301–311.
38. Karp JM and GS Leng Teo. (2009). Mesenchymal stem cell homing: the devil is in the details. Cell Stem Cell 4: 206–216.

Address correspondence to:
Dr. Songlin Wang
Molecular Laboratory for Gene Therapy and Tooth Regeneration
Beijing Key Laboratory of Tooth Regeneration and Function Reconstruction
Capital Medical University School of Stomatology
Tian Tan Xi Li No.4
Beijing 100050
People's Republic of China

E-mail: slwang@ccmu.edu.cn

Songtao Shi
The Center for Craniofacial Molecular Biology
Herman Ostrow School of Dentistry
University of Southern California Los Angeles
Los Angeles, CA 90033

E-mail: songtaos@usc.edu

Received for publication December 14, 2012
Accepted after revision January 30, 2013
Prepublished on Liebert Instant Online January 30, 2013